AUT Journal of Mechanical Engineering

AUT J. Mech. Eng., 4(4) (2020) 427-434
DOI: 10.22060/ajme.2020.16951.5843

# Prediction of Flow Behavior and Level of Hemolysis in a Pulsatile Left Ventricular Assist Device

A. H. Vakilzadeh, K. Javaherdeh*

Faculty of Mechanical Engineering, University of Guilan, Rasht, Iran

**ABSTRACT:** Heart failure claims the lives of thousands of people annually. Left ventricular assist device is a valid treatment option for patients with an advanced stage of heart failure. The left ventricular assist device is a blood pump increasing the pumping ability of the bottom left chamber of the patient's heart. In this study, we investigate the hemolytic characteristics of a left ventricular assist device. The main objective of this paper is to explore the effects of amplitude and frequency on levels of hemolysis via computational fluid dynamic in an implantable reciprocating pump. Thus, the dynamic mesh technique is utilized to simulate piston motion and valves closure. Moreover, a system of time-dependent nonlinear partial differential equations is coupled with each other to predict blood flow and hemolysis index. Fluid dynamic characteristics are obtained by employing continuity and momentum equations and the levels of hemolysis are also calculated by applying two additional scalar transport equations based on an Eulerian transport approach. The results depicted the favorable reduction in hemolysis index by increasing frequency and decreasing amplitude simultaneously at specific Reynolds number, they also showed that the average hemolysis at the right side of the piston is slightly higher than the left side and it obtains its maximum value at valves and clearance domains.

**Review History:**
Received: Aug. 22, 2019
Revised: Oct. 06, 2019
Accepted: Dec. 09, 2019
Available Online: Jan. 04, 2020

**Keywords:**
Left ventricular assist device
Blood pump
Hemolysis
Eulerian transport approach
Dynamic mesh

## 1- Introduction

Heart disease is the outstanding reason for fatality in the world [1]. Amid all diseases related to heart, millions of people in western countries [2], more than 16 million people in Europe and the United States are afflicted with Heart Failure (HF), where its prevalence is about 2.5% of the normal population [3]. The effective therapy of the most advanced stage of HF can be cardiac transplantation but unfortunately, there are not adequate donor numbers for the patients awaiting heart transplantation such that many of them die on the waiting list due to heart donor shortage. Thus, a lot of requirements for finding alternative therapy led to developing Ventricular Assist Devices (VADs) [5]. The VADs are electromechanical blood pumps utilized for assisting weakened heart function as long- and short-term supports [6]. In the long-term VAD, the patient will survive outside of the hospital with an accepTable condition until a heart transplant becomes available. The VAD can help the left ventricle (Lift Ventricular Assist Device (LVAD)) or the right ventricle, or both devices are used simultaneously to support both ventricles. As a high percentage of HF is related to left ventricular insufficiency, using an implanTable LVAD has attracted the attention of many HF patients such that about 2500 LVADs were implanted in patients with acute HF in the USA in 2013 [7]. This VAD works with the heart and helps it to pump more blood with less work by receiving blood from the left ventricle and sending it to the aorta. This device is categorized into three generations. The first generation was pulsatile volume displacement pumps driven by a pneumatic or electric drive system. The second generation includes rotary-pump designs providing continuous flow and have bearings to support rotors; these probably fail due to wear which results in undesirable performance or device stopping. The third generation is a centrifugal and axial pump with rotors supported totally by magnetic levitation [8]. This kind of support minimizes wear by preventing direct contact between components. Although potential benefits of LVAD with Continuous Flow (CF LVAD) have led to the widespread use of these devices as a useful option for helping patients with a weakened heart ventricle, because of not being physiologic (reduced pulsatility), there are concerns about possible dangers of non-pulsatile blood flow. Reducing arterial pulse pressure and flow at constant pump speed and occurrence of cardiovascular diseases such as aortic insufficiency, gastrointestinal bleeding, and right HF have been reported for CF LVAD device [9]. Conversely, Pulsatile Flow LVADs (PF LVAD) enhance the likelihood of myocardial recovery, kidney performance, and blood flow of vital organs [10]. Since in PF LVAD, the increment of coronary artery perfusion is more considerable than CF LVAD, the produced hemodynamic energy is significantly higher [11]. Moreover, because of not needing valves in CF LVAD, a mechanical failure leads to severe aortic insufficiency [12]. As mentioned previously,

*Corresponding author's email: javaherdeh@guilan.ac.ir

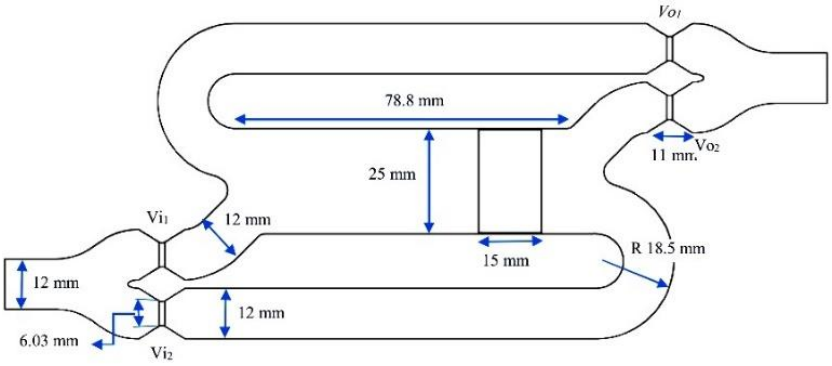


**Fig. 1. Planar configuration of the blood pump**

many patients have benefitted from VADs so far, nevertheless, the VADs have the potential to help many more patients provided that blood damage problems in the blood pump, the most important component of the VADs, are minimized. The main blood damage includes hemolysis and thrombosis. Releasing damaged red blood cells hemoglobin into the plasma is known as hemolysis. This free hemoglobin has different negative effects, it is toxic for the kidneys which can lead to adverse clinical outcomes and kidney dysfunction [13], it also pollutes the blood plasma and decreases the level of blood hematocrit (the volume percentage of red blood cells in the blood) [14]. Thus, the blood pumps should be designed in such a way that the possibility of hemolysis is minimized. The degrees of thrombosis, clot formation and hemolysis depend on physiological conditions, the biocompatibility of the blood-contacting surface, and the fluid mechanics of blood flow in the blood pump [15]. Hence, the detailed understanding of the flow inside the pump and investigating hemolysis which depends on the level of shear stress acting on the cell and exposure time of that shear stress are essential to avoid or minimize blood damage and appraising pump performance. To evaluate red blood cell damage in blood flows, many models have been presented so far. The most widely used model is a power-law model developed by Giersiepen et al. [16] from empirical observation. They demonstrated that the ratio of released hemoglobin into the plasma to the total hemoglobin ($H=\frac{\Delta HB}{HB}$), damage index, is a power-law function of shear stress and exposure time [17]. Generally, based on this model, two types of computational methods are available to evaluate hemolysis via Computational Fluid Dynamics (CFD): Lagrangian and Eulerian approaches. In the Lagrangian approach, hemolysis is estimated by tracking particles along path lines and integrating shear stress and exposure time along with them [18]. Notably, the path lines which are followed from the inlet of a device to the outlet may not cover the whole flow domain. Specifically, areas of high potential damage, such as recirculation zones and boundary layers, may not be passed by any path line, which may result in underestimating hemolysis prediction. In the Eulerian approach, the damage index is integrated over the entire computational flow domain, hence, we can identify areas that are susceptible to blood damage. This method predicts hemolysis by utilizing transport equations within the reference frame of the CFD solver, that is, simultaneously with solving continuity and momentum equations, the hemolysis calculation is performed [19]. In this paper, we focus on the hemolysis part of blood damage in a pulsatile blood pump. Unlike the previous works at which Eulerian methods were just used to evaluate hemolysis in continuous blood pumps, this study applies the Eulerian transport approach in the pulsatile blood pump. Thus, levels of hemolysis in all parts of the pump are determined. To the authors' knowledge, exploring hemolysis in detail in a reciprocating blood pump is a novel work. The designed pump for this study is according to a magnetically suspended reciprocating pump proposed by Di Paolo et al. [12]. The effects of amplitude and frequency on the level of hemolysis in a laminar regime is investigated by simulating piston motions and valves closure with a dynamic mesh technique.

## 2- Computational Methods and Procedures

The schematic of the pump was shown in Fig. 1. As it can be seen, it includes four valves and one moving piston. $Vi_1$ and $Vi_2$ are suction valves and $Vo_1$ and $Vo_2$ are discharge valves. In each moment, two valves are opened and two other ones are closed, i.e., by moving the piston toward the left, while $Vi_1$ and $Vo_2$ are closed, pump suctions blood via $Vi_2$ and discharges it via $Vo_1$. Conversely, as soon as the piston reaches the end of the cylinder and changes its direction, the closing valves ($Vi_1$ and $Vo_2$) are opened and the opening ones ($Vi_2$ and $Vo_1$) are closed. This computational fluid dynamics study is carried out to assess the flow conditions in the blood pump and characterize flow-induced stress resulting in red blood cell damage. Unsteady simulation in laminar regime is performed for blood flow in the pump with a planar configuration. Since the shear rates found in VADs are high [4] (>100 1/s), in line with other researchers, in this study blood is considered as an incompressible Newtonian fluid with a density of 1030 kg/m$^3$ and dynamic viscosity of 3.5 MPa.s [20]. A dynamic mesh method is applied to model the motion of the piston and valve closure. The hemolysis index is calculated following Yu et al. [19]. Thereby, the damage experienced by the blood on its way through the pump is integrated using a new Eulerian

formulation. That way, two advection equations are coupled with continuity and momentum equations. The numerical simulations are conducted utilizing the commercial, finite elements software COMSOL Multiphysics 5.2a. Time-dependent solver with fully coupled algorithm and PARDISO solver is selected to solve sets of incompressible coupled nonlinear partial differential equations. The fully coupled approach forms a single system of equations that are solved for all of the unknowns and includes all of the couplings between the unknowns at once, within a single iteration. This solver starts from an initial guess and applies Newton-Raphson iterations until the convergence of solution within the required prescribed error tolerance. In this paper, the absolute tolerance is set to 0.0001 to control the largest allowable absolute error at any step. Time derivatives are discretized with implicit Backward Difference Formula (BDF) with an order of accuracy varying from one (minimum BDF order) to two (maximum BDF order). Each calculation took about 6 days to converge. In the following, the method of investigating is discussed in detail.

### 2-1- Flow calculation

In this section, the governing equations applied to obtaining flow field and hemolysis index in the pump are presented. Blood flow is modeled by the momentum and mass conservation equations for an incompressible fluid,

$$\frac{\partial u_i}{\partial x_i} = 0 \tag{1}$$

$$\frac{\partial u_i}{\partial t} + u_j \frac{\partial u_i}{\partial x_j} = -\frac{1}{\rho}\frac{\partial p}{x_i} + \frac{\partial}{\partial x_j}\upsilon\frac{\partial u_i}{\partial x_j} \tag{2}$$

where $u$ is velocity, $p$ denotes pressure, $v$ is dynamic viscosity and $\rho$ is the fluid density. It should be noted that *P2 + P1* elements are used for discretization of fluid, i.e., second-order elements for the velocity components and linear elements for the pressure field are implemented. The boundary condition at the inlet is a pressure inlet with a pressure of zero and at the outlet, a pressure outlet is defined with 100 mmHg (mean aortic pressure). Additionally, moving wall boundary condition is considered for piston wall and all four valves as following:

Here, $f$ and $A$ represent frequency and amplitude of the piston, respectively. $M$ and $\beta$ are constant numbers that determine the intensity and sharpness of valve suddenly motions.

$$u_w = -2\pi f A \sin(2\pi f t) \qquad \text{Piston wall} \tag{3}$$

Valve (upper wall) (4)

$$v_{wallup} = \begin{cases} 15M\times(\cosh(x)-\sinh(x)) & \sin(2\pi ft)\geq 0 \\ -15M\times(\cosh(x)-\sinh(x)) & \sin(2\pi ft)\leq 0 \end{cases} \qquad x = \left[\beta\left(t-\frac{1}{2f}\right)\right]^2$$

$$v_{\text{bottom wall}} = -v_{\text{upper wall}} \qquad \text{Valve (bottom wall)} \tag{5}$$

### 2-2- Hemolysis calculation

To evaluate hemolysis in time-dependent shear conditions using a power-law approach, Yu et al. [19] base on Lagrangian formulation considering blood cell damage history, proposed an Eulerian model to predict hemolysis index following Eqs. (6) and (7):

$$\frac{\partial D_b}{\partial t} + (V.\nabla) D_b = \tau^{\frac{\alpha}{\beta}} \tag{6}$$

$$\frac{\partial H_L}{\partial t} + (V.\nabla) H_L = c\beta D^{\beta-1}\tau^{\frac{\alpha}{\beta}} \tag{7}$$

Here, $D_b$ is mechanical dose and $H_L$ is defined as a scalar variable equal to $H^{1/\beta}$, where $H$ denotes the ratio of plasma free hemoglobin to total blood hemoglobin ($H=\frac{\Delta HB}{HB}$), $c$, $\alpha$, and $\beta$ are the empirical constants derived by different authors based on experimental data. In this study, the constants proposed by Heuser and Opitz [21] are applied ($c$=1.8×10$^{-8}$, $\alpha$=1.991, $\beta$=0.765). $\tau$ is scalar shear stress calculated according to the method proposed by Bludszuweit as follows [16]:

$$\tau = \left(\tau_{xx}^2 - \tau_{xx}\tau_{yy} + \tau_{yy}^2 + 3\tau_{xy}^2\right)^{\frac{1}{2}}, \quad \tau_{ij} = \mu\frac{\partial u_i}{\partial x_j} \tag{8}$$

The scalar shear stress components are derived from the velocity field obtained from the numerical simulations of the blood flow. Scalar quantity and scalar flux are determined to be zero as boundary conditions at the inlet and all solid walls, respectively. The ultimate hemolysis ratio is calculated by mass-weighted averaging of $H$ at the outlet of the pump (hemolysis index). Moreover, as COMSOL Multiphysics is based on the finite element method when the element Peclet number exceeds 1, the approach leads to numerical instabilities. Thus, for advection transport equations like Eqs. (6) and (7), the crosswind stabilization method [22] is used to prevent this phenomenon.

## 3- Validation and Mesh Convergence Analysis

To perform grid independence study, hemolysis index and averaged flow rate for three meshes with the same structure and different maximum element sizes are calculated at a frequency of 4.25, the amplitude of 20 mm, and clearance of 0.1 mm. The difference between the finest (468254 elements) and the next coarser (373997 elements) grids was only 1% in average flow rate and 2.5% in hemolysis index. Therefore, the selected and final mesh consisted of 373997 elements. The quad elements with maximum element size equal to 0.00015 are utilized for the valves zones, and clearance and other regions are meshed using triangular elements with maximum element size equal to 0.00004 and 0.00045, respectively. It should be noted that the reasonable mesh structure obtained under these conditions will also be used for other conditions. Moreover, before performing CFD, the validity of the computational model is checked. Therefore, firstly, under given conditions, we obtain the profile of

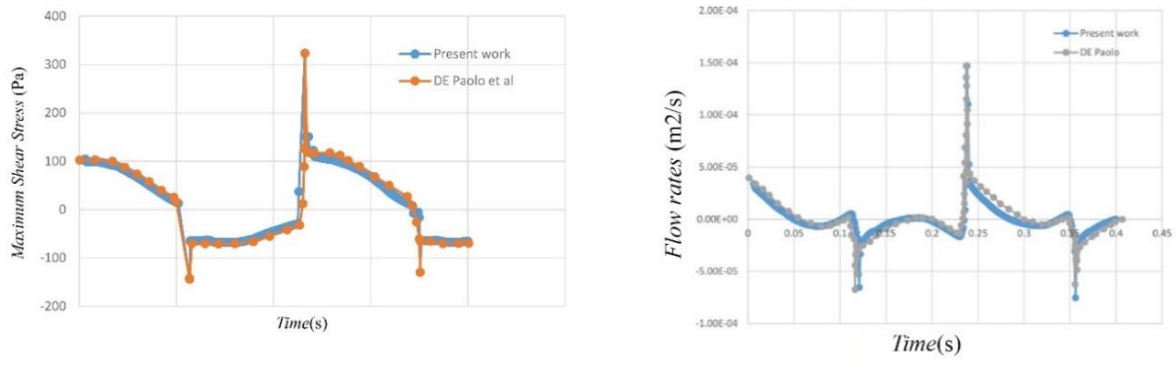


(a) (b)

**Fig. 2. Comparison of predicted and Di Paolo et al. [12] results (a) maximum shear stress (b) flow rate into clearance**

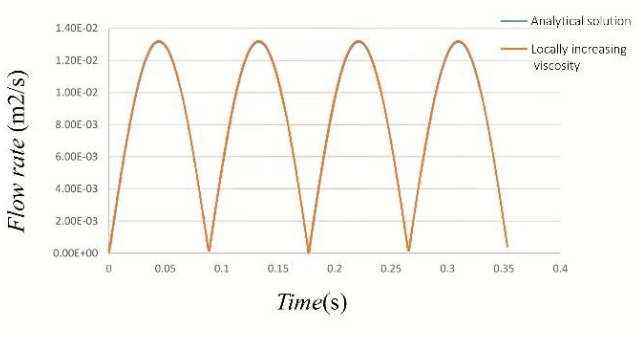


**Fig. 3. Comparison of Outlet flow rate profiles between analytic and numeric results during two periods at $f$= 4.25 Hz, $A$= 20 mm, and $C$= 0.1 mm**

Maximum Shear Stress (MSS) and flow rates into clearances between piston and housing with dynamic mesh technique and compare them with the study conducted by Di Paolo et al. [12]. Secondly, the volumetric flow rate at pump output over two periods with locally augmenting viscosity method, considering high viscosity for fluid (order of 104) in the instances that valves need to be closed, and analytical solution is acquired, then the obtained result compare with each other. In a positive displacement pump, flow rate is directly related to the stroke volume and the pumping frequency. Thus, by considering the velocity of the piston, i.e., $A\omega\sin(\omega t)$ and applying continuity equation, the flow rate at the output is obtained as follow:

$$Q = A\omega h\sin(\omega t) \tag{9}$$

where Q is the volumetric flow rate, ω is angular velocity and h is the height of the piston.

As it can be seen in Fig. 2, the present results have good agreement with results from Di Paolo et al. [12] so that the profile of maximum shear stress obtained in this study is overlapped with the results of Di Paolo et al. [12]. Regarding clearance flow rate, the trend of the present study is similar to Di Paolo et al. [12] results, the only difference is related to the peak of negative flow rate which is less than 3%. Additionally, Fig. 3 shows the two line graphs obtained analytically and numerically are compatible. These agreements demonstrate the validity and precision of the numerical procedure.

## 4- Results and Discussion

In this section, firstly, the simultaneous influence of amplitude and frequency on flow dynamics and hemolysis at a specific Reynolds number at which the minimum required flow rate to do most daily activities (5 Lit/min) is satisfied, are explored. Secondly, we investigate pump behavior completely at a certain frequency and amplitude. Notably, to prevent the mesh from collapsing in the closed valves, the existence of a very small gap in these zones which leads to little leakage flow is inevitable. Generally, the effect of various amplitudes and frequencies at specific Reynolds number on hemolysis production and streamline patterns are explored as follow.

### 4-1- Investigating the effect of amplitude and frequency on hemolysis

Since Reynolds number depends on kinematic viscosity of fluid, amplitude, and frequency of piston, firstly, in laminar flow, to investigate the effect of amplitude and frequency at specific Reynolds number, the values of these parameters are modified simultaneously to make the multiplication of them constant and as a result, Reynolds number does not change. Di Paolo et al. [12] showed that in A=20 mm and f=4.25 Hz (A×f =85) the flow is laminar and the minimum required flow rate is produced with pump. Thus, the values of these two parameters are chosen in such a way that the result of their multiplication is equal to 85 as shown in Table 1.

The hemolysis index for three cases of Table 1 is shown in Fig. 4(a). As it can be seen, by increasing frequency and decreasing amplitude simultaneously the hemolysis index decreases favorably. At certain A×f, as the frequency increases by 10% from case 3 to case 2, red blood cell damage index is decreased by 13.8% and with a 33 percent increase in frequency from case 2 to case 3, interestingly hemolysis index is reduced more than four times. This is because of the time lag to exit blood from the pump. It means the pump needs a time interval to produce the required pressure so that at a higher frequency and lower amplitude, a lower time lag is observed.

**Table 1. Three different amplitudes and frequencies**

| Case No. | $A$ [mm] | $f$ [Hz] | $A \times f$ |
|---|---|---|---|
| Case 1 | 15 | 5.65 | 85 |
| Case 2 | 20 | 4.25 | 85 |
| Case 3 | 22 | 3.87 | 85 |

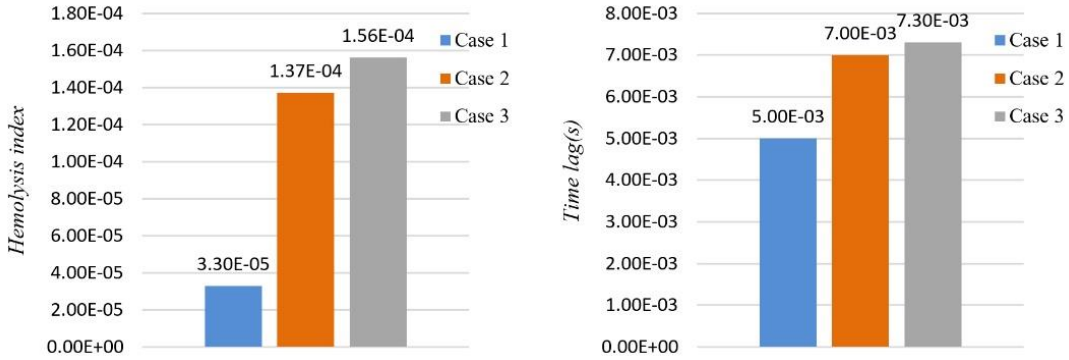


(a) (b)

**Fig. 4. (a) Hemolysis index and (b) Time lag for three cases of Table 1**

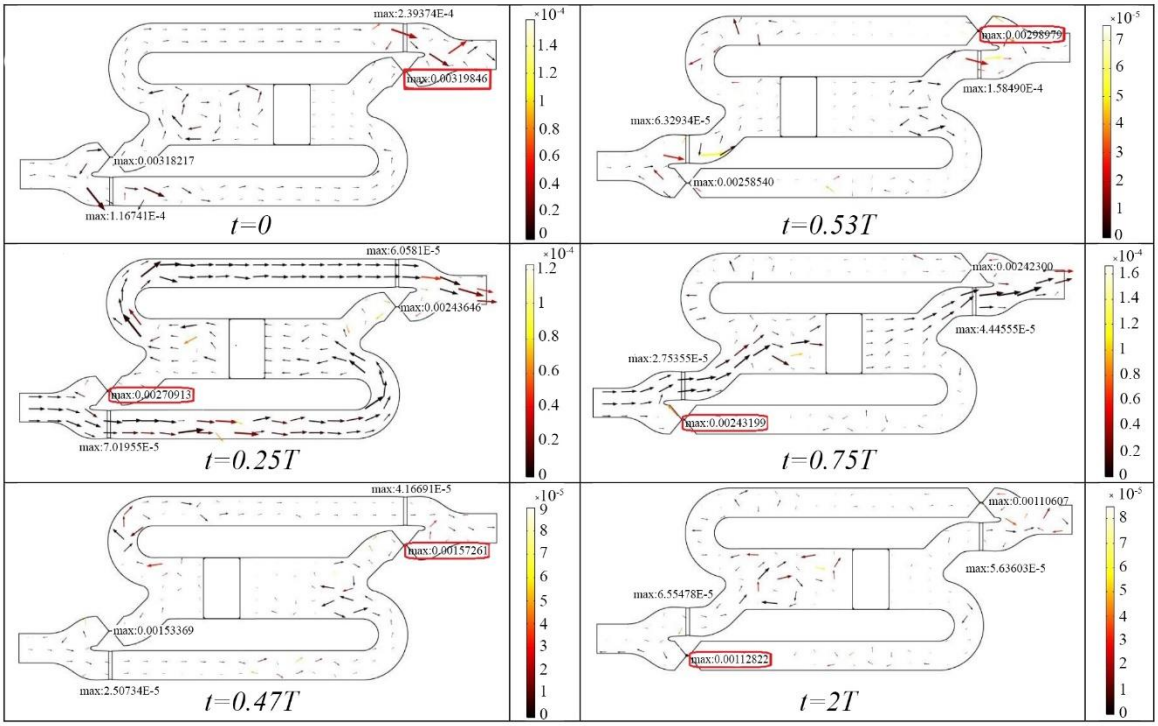


**Fig. 5. Velocity vectors and values of hemolysis at $f$=5.65 Hz and $A$=15 mm during one period**

This feature is depicted in Fig. 4(b). As shown, it decreases about 2.5 milliseconds with augmentation of the frequency from 5.65 to 3.86. Since the hemolysis index in case 1 was lower than other ones, in the following of this section, the behavior of pump at a frequency of 5.65 Hz with an amplitude of 15 mm at clearance 0.1 mm (Case 1) is analyzed. Thus, velocity field, average and maximum hemolysis in all parts of pump, and path lines in the pump for the time-averaged motion over one period are obtained.

Fig. 5 shows velocity vectors and values of hemolysis under the given conditions during one period (third period) at six different instances. In this Figure, the length and the color of each vector indicate the magnitude of velocity and hemolysis value, respectively. It is also depicted the location of maximum hemolysis in all valves and domain. The circulation zone in front of the piston is formed at the initial steps and

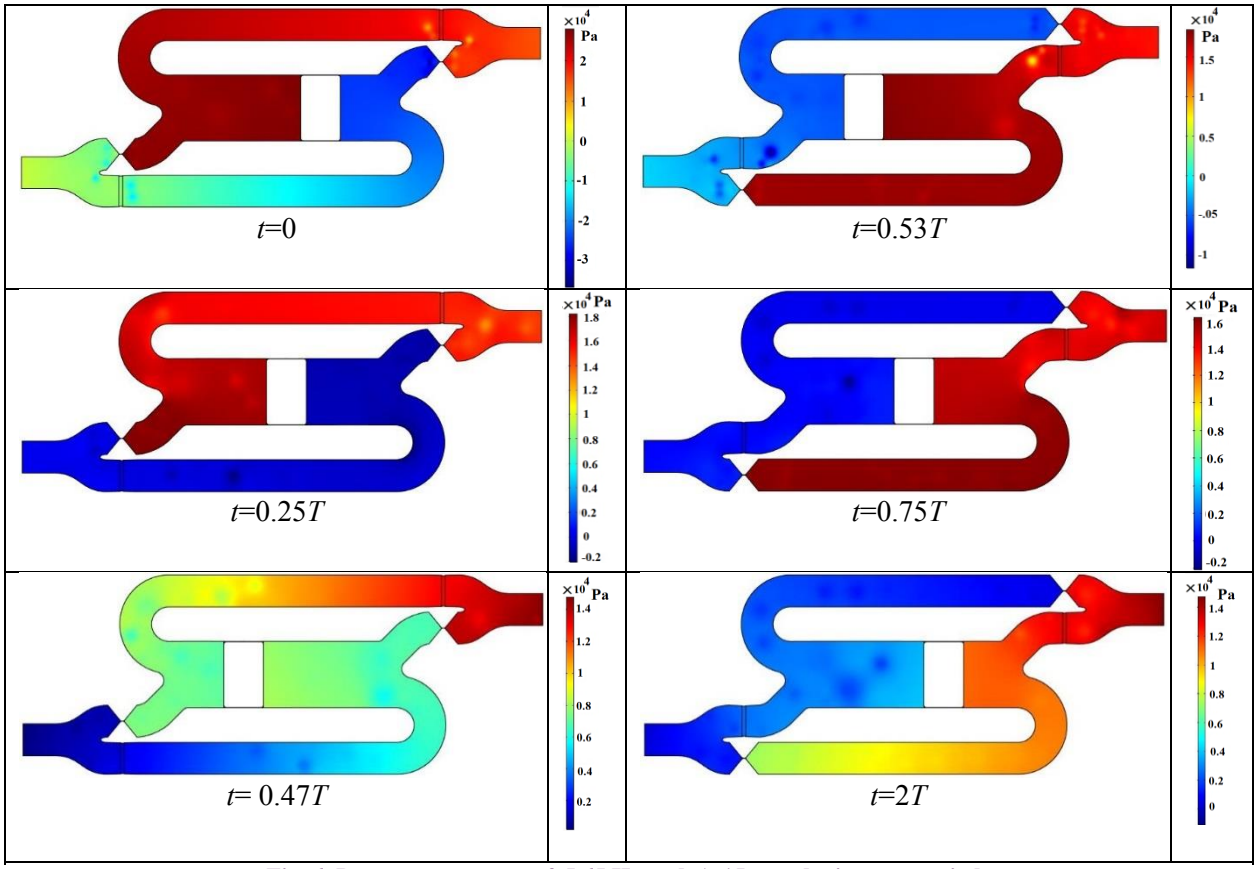


**Fig. 6. Pressure contour at *f*=5.65 Hz and *A*=15 mm during one period**

disappeared by moving the piston toward the center of the cylinder (steps 2 and 4). It should be noted that suction of fluid at the previous half period as shown in steps 3 and 6 leads to forming these unstable circulation flows in the pump. The sudden closure of the valves causes another circulation region at the sides of these valves. Also, there are flow separations in bends to change the fluid flow direction. By moving the piston toward the center, a uniform flow pattern with higher velocity and the lowest circulation zone is produced in almost entire domain (step 2). Turning to hemolysis, the lighter the color of vectors is, the higher value of the hemolysis index is. The high hemolysis region is observed in the circulation flow region appeared on the sides of the piston and closed valves. With this Figure, it is clear that the color of vectors in the vicinity of closed valves are much lighter at all steps indicating the highest hemolysis occurs in this area. Furthermore, hemolysis due to flow separation in the bends is insignificant and can be neglected in comparison with created hemolysis in valve areas. Besides, the maximum values of hemolysis ($H_{max}$) in all valves are obtained and depicted in Fig. 5. As it is illustrated, the $H_{max}$ (shown in a red box) decreases from 0.003198 (step 1) to 0.001572 (step 3) during the first half period. A similar pattern is seen for the second half period at which the $H_{max}$ reduces from 0.00298 (step 4) to 0.001128 (step 6). This deviation can result from the difference in the distance traveled by the fluid in two half periods of motion.

Fig. 6 illustrates the pressure contour of the blood pump at f=5.65 Hz and $A$=15 mm during one period. As it can be seen, the motion of the piston causes the pressure in one chamber to go beyond the $P_{out}$ and simultaneously in the other chamber, to fall below the $P_{in}$. Consequently, the blood can enter the pump from the inlet and fills it, and eject through the output. To understand the influence of pump conFiguration on hemolysis, the pump is divided into seven subdomains namely Inlet Domain (ID), Right Chamber (RC), Left Chamber (LC), inlet Valves (Vi), outlet Valves (Vo), and Outlet Domain (OD). To this end, the value of average hemolysis ($H_{avg}$) for all subdomains is obtained and depicted in Fig. 7. As illustrated, $H_{avg}$ in ID, RC, and LC domains is of order $1e^{-6}$ and for others, it becomes further one order of magnitude ($1e^{-5}$). Moreover, it is obvious that when the piston moves toward the left the fresh blood flows into RC (bottom channel) through valve Vi2 but with changing piston movement direction, fresh blood enters the LC directly. Thus, the right side of the piston always exposes to the blood of the previous period whereas the other side is relatively in contact with fresh blood entering the pump in current period from valve Vi1. As a result, the value of $H_{avg}$ is expected to be slightly higher for RC. As expected, $H_{avg}$ in valves and clearance subdomains is higher compared with others. It is observed, the highest value of $H_{avg}$ happens at Vo, which is equal to 2.85e-5 and it is minimal in the inlet region.

Moreover, the $H_{avg}$ value in outlet valves is higher than inlet one. This can be because of passing the blood from inlet valves, LC, and RC domains (Vi1 and Vi2) to reach outlet

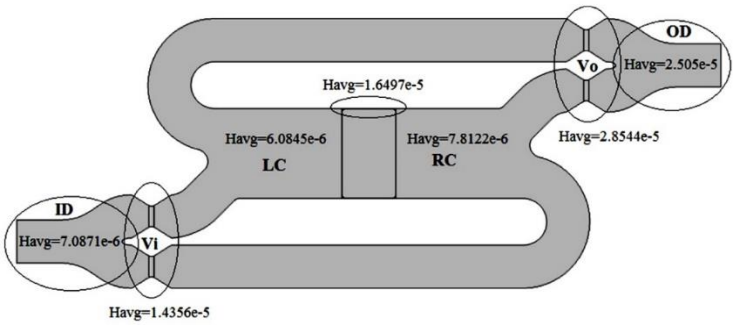


**Fig. 7. The average value of hemolysis in seven subdomains at *f*=5.65 Hz, *A*=15mm and *C*=0.1 mm**

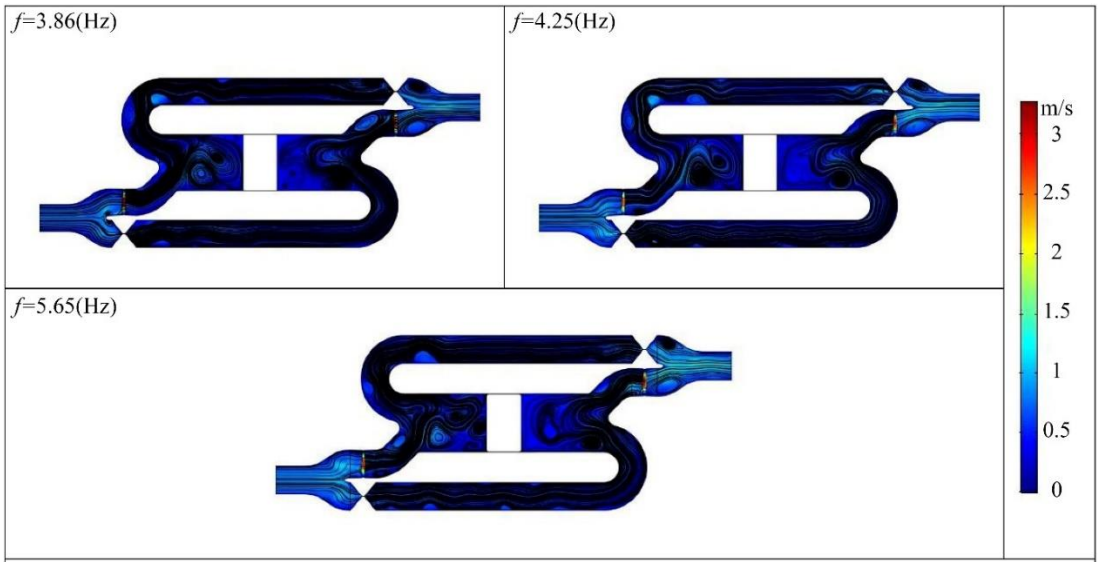


**Fig. 8. Contours of velocity magnitude and path lines in the pump for the time averaged motion over one period in dynamic mesh method**

valves (Vo1 and Vo2). Besides, it is also illustrated, $H$ and $H_{avg}$ acquire their maximum values in the same location at Vo. This is due to valve movement and little leakage flow of closed valve. Fig. 8 illustrates the contour of velocity magnitude and the path lines in the pump for the time-averaged motion over one period (third period). This Figure is obtained for different cases in Table 1 by applying the dynamic mesh technique. As can be seen, the mean velocity of all cases is similar and varies in the range of 0 to 3 m/sec which the maximum values occur in the valves domain. In all cases, two symmetric vortices with the same patterns are generated in the OD. Also, in the top and bottom channels, approximately parallel path lines are observed. It is seen, the two vortices forming at the elbows of outlet directions of RC and LC are disappeared by increasing the frequency. This indicates that the increment of momentum leads to postponing the separation of the boundary layer in these areas. At the lowest frequency, two small vortices which are produced at ID location in the two branches of the fluid flow path are completely vanished and transferred to the LC with stronger strength by increasing frequencies. Fig. 8 also shows that because of the reciprocation motion of the piston in the cylinder, in all frequencies most vortices are formed in this area.

## 5- Conclusions

In this paper, we investigated behavior of a blood reciprocating pump with a planar conFiguration. To this end, the effects of frequency and amplitude on red blood cell damage were explored. The damage that is experienced by the blood on its way through the pump was integrated using a new Eulerian formulation proposed by Yu et al. [19]. Additionally, valves and piston motions were simulated with the dynamic mesh technique. Average hemolysis at different parts of the pump was acquired at A=15 mm, f=5.65 Hz, and C=0.1 mm. Moreover, the hemolysis index at the outlet of the pump was calculated for three different values of amplitude and frequency at a specific Reynolds number to study the simultaneous influence of these two parameters on pump behavior. Finally, path lines in the pump for the time-averaged motion over one period for all cases of Table 1 were obtained. The main results of this paper are summarized as follows:

I) Increasing frequency and reducing amplitude simultaneously decrease the time lag, and consequently, reduce the hemolysis index.

II) At specific frequency and amplitude, by increasing clearance size, time lag increases, and a circulation zone with

a higher jet flow rate at the back of the piston forms which increases hemolysis value at clearance domain and pump outlet, so that the hemolysis value at outlet and clearance region becomes approximately 1.5 times and more than 2.5 times from case 4 to case 6, respectively.

III) $H_{avg}$ is minimal in the inlet region and obtained its maximum value at valves and clearance subdomains. Besides, since the right side of the piston always exposes to the blood of the previous period and the other side is relatively in contact with fresh blood entering the pump in the current period from valve Vi1, the value of $H_{avg}$ at RC is slightly higher than LC.

In the end, we note that although the hemolysis index is low at a higher frequency and lower amplitude since flow rate varies linearly with frequency, by doubling the thickness of the pump, its frequency is halved.

## NOMENCLATURE

| | | | |
|---|---|---|---|
| $A$ | amplitude of piston movement | $P$ | pressure |
| $C$ | clearance size | $Q$ | volumetric flow rate |
| $c$ | empirical constant | $t$ | time |
| $f$ | frequency of piston movement | $u$ | velocity |
| $h$ | piston height | $\alpha, \beta$ | empirical constants |
| $H$ | hemolysis index | $\mu$ | dynamic viscosity of fluid |
| $HB$ | total blood hemoglobin | $\rho$ | density of fluid |
| $\Delta HB$ | plasma free hemoglobin | $\tau$ | scalar shear stress |
| $H_L$ | a scalar variable equal to $H^{1/\beta}$ | $v$ | kinematic viscosity |
| | | $\omega$ | angular velocity |

## REFERENCES


[1] M. Alizadeh, S. Rahmani, P. Tehrani, Calculating the aortic valve force and generated power by a specific cardiac assist device (AVICENA) in different counterpulsation, Journal of the Brazilian Society of Mechanical Sciences and Engineering, 40(6) (2018) 286.

[2] J. Garbade, H.B. Bittner, M.J. Barten, F.-W. Mohr, Current trends in implantable left ventricular assist devices, Cardiology research and practice, 2011 (2011).

[3] A.T. Tzallas, N.S. Katertsidis, E.C. Karvounis, M.G. Tsipouras, G. Rigas, Y. Goletsis, K. Zielinski, L. Fresiello, A. Di Molfetta, G. Ferrari, Modeling and simulation of speed selection on left ventricular assist devices, Computers in biology and medicine, 51 (2014) 128-139.

[4] K. Fraser, M. Taskin, T. Zhang, B. Griffith, Z. Wu, Comparison of shear stress, residence time and lagrangian estimates of hemolysis in different ventricular assist devices, in: 26th Southern Biomedical Engineering Conference SBEC 2010, April 30-May 2, 2010, College Park, Maryland, USA, Springer, 2010, pp. 548-551.

[5] C. Long, M. Esmaily-Moghadam, A. Marsden, Y. Bazilevs, Computation of residence time in the simulation of pulsatile ventricular assist devices, Computational Mechanics, 54(4) (2014) 911-919.

[6] S. Rahmani, M. Navidbakhsh, M. Alizadeh, Investigation of a new prototype of multi-balloons LVAD using FSI, Journal of the Brazilian Society of Mechanical Sciences and Engineering, 40(1) (2018) 8.

[7] J.N. Kirkpatrick, G. Wieselthaler, M. Strueber, M.G.S.J. Sutton, J.E. Rame, Ventricular assist devices for treatment of acute heart failure and chronic heart failure, Heart, 101(14) (2015) 1091-1096.

[8] C.A. Thunberg, B.D. Gaitan, F.A. Arabia, D.J. Cole, A.M. Grigore, Ventricular assist devices today and tomorrow, Journal of cardiothoracic and vascular anesthesia, 24(4) (2010) 656-680.

[9] K.G. Soucy, G.A. Giridharan, Y. Choi, M.A. Sobieski, G. Monreal, A. Cheng, E. Schumer, M.S. Slaughter, S.C. Koenig, Rotary pump speed modulation for generating pulsatile flow and phasic left ventricular volume unloading in a bovine model of chronic ischemic heart failure, The Journal of Heart and Lung Transplantation, 34(1) (2015) 122-131.

[10] L. Xu, M. Yang, L. Ye, Z. Dong, Computational fluid dynamics analysis and PIV validation of a bionic vortex flow pulsatile LVAD, Technology and Health Care, 23(s2) (2015) S443-S451.

[11] B. Cremers, A. Link, C. Werner, H. Gorhan, I. Simundic, G. Matheis, B. Scheller, M. Böhm, U. Laufs, Pulsatile venoarterial perfusion using a novel synchronized cardiac assist device augments coronary artery blood flow during ventricular fibrillation, Artificial organs, 39(1) (2015) 77-82.

[12] J. Di Paolo, J.F. Insfrán, E.R. Fries, D.M. Campana, M.E. Berli, S. Ubal, A preliminary simulation for the development of an implanTable pulsatile blood pump, Advances in biomechanics and applications, 1(2) (2014) 127-141.

[13] M. Behbahani, M. Behr, M. Hormes, U. Steinseifer, D. Arora, O. Coronado, M. Pasquali, A review of computational fluid dynamics analysis of blood pumps, European Journal of Applied Mathematics, 20(4) (2009) 363-397.

[14] A. Schenkel, M. Deville, M. Sawley, P. Hagmann, J.-D. Rochat, Flow simulation and hemolysis modeling for a blood centrifuge device, Computers & Fluids, 86 (2013) 185-198.

[15] E. Okamoto, T. Hashimoto, T. Inoue, Y. Mitamura, Blood compatible design of a pulsatile blood pump using computational fluid dynamics and computer-aided design and manufacturing technology, Artificial organs, 27(1) (2003) 61-67.

[16] M. Giersiepen, L. Wurzinger, R. Opitz, H. Reul, Estimation of shear stress-related blood damage in heart valve prostheses-in vitro comparison of 25 aortic valves, The International journal of artificial organs, 13(5) (1990) 300-306.

[17] K.H. Fraser, M.E. Taskin, B.P. Griffith, Z.J. Wu, The use of computational fluid dynamics in the development of ventricular assist devices, Medical engineering & physics, 33(3) (2011) 263-280.

[18] O. Myagmar, S.W. Day, The evaluation of blood damage in a left ventricular assist device, Journal of Medical Devices, 9(2) (2015) 020914.

[19] H. Yu, S. Engel, G. Janiga, D. Thévenin, A review of hemolysis prediction models for computational fluid dynamics, Artificial organs, 41(7) (2017) 603-621.

[20] M.E. Taskin, K.H. Fraser, T. Zhang, B. Gellman, A. Fleischli, K.A. Dasse, B.P. Griffith, Z.J. Wu, Computational characterization of flow and hemolytic performance of the UltraMag blood pump for circulatory support, Artificial organs, 34(12) (2010) 1099-1113.

[21] G. Heuser, R. Opitz, A Couette viscometer for short time shearing of blood, Biorheology, 17(1-2) (1980) 17-24.

[22] C. Multiphysics, Comsol multiphysics user guide (version 4.3 a), COMSOL, AB, (2012) 39-40.



**HOW TO CITE THIS ARTICLE**

*A.H. Vakilzadeh, K. Javaherdeh. Prediction of Flow Behavior and Level of Hemolysis in a Pulsatile Left Ventricular Assist Device. AUT J. Mech Eng., 4(4) (2020) 427-434.*

**DOI:** 10.22060/ajme.2020.16951.5843